and for $n < N - 1$

$$r_{CC}(n) = 1 + \sum_{l=1}^{N-n-1} J^* \begin{bmatrix} 1 & 0 \\ 0 & 0 \end{bmatrix} \prod_{i=1}^{j} U_{n+i+1} \cdot \begin{bmatrix} 0 & \tau_{n+j+2} w^l \prod_{i=2}^{l} SM_{n+j+i+1} \\ 0 & 0 \end{bmatrix} \begin{bmatrix} 0 & 0 \\ \mathcal{S}^{\alpha}_{n+j+2+l} & 0 \end{bmatrix} \prod_{i=n+j+3+l}^{N} U_i J \quad \text{(B-18)}$$

wherein $\prod_{i=\beta}^{\alpha} \mathbf{U}_i = \mathbf{E}$ if $\alpha < \beta$ and $\mathcal{S}^{\alpha}_{n+j+2+l} = \mathcal{S}_{n+j+2+l}$ if $n + j + 2 + l \leq N$ and equals one otherwise: the "1" in eq B-18 is the statistical weight of the $N - n$ block completely randomly coiled state.

For a homopolymer we have

$$r_{CC}(n) = 1 + \sum_{l=1}^{N-n-1} \tau w^l S M^l \mathcal{S}^{\alpha}_{n+j+2+l} U_{11}{}^{j} [U_{11}{}^{N-n-j-2-l} + U_{12}{}^{N-n-j-2-l}] \quad \text{(B-19)}$$

wherein $\mathbf{U}^{\alpha}$ is, as previously, given in eq A-9a and A-9b.

Finally, if r_{HC} is the statistical weight of all the allowed conformations of blocks $n + 1, \ldots, N$ on chain two when block n is helical and block $n + 1$ is a random coil, it can be shown that

$$r_{HC}(n) = \mathcal{S}_{n+1} r_{CC}(n) \quad \text{(B-20)}$$

References and Notes

(1) Skolnick, J.; Holtzer, A. *Macromolecules* **1982**, *15*, 303.
(2) (a) Skolnick, J.; Holtzer, A. *Macromolecules* **1982**, *15*, 812. (b) Holtzer, M. E.; Holtzer, A.; Skolnick, J. *Macromolecules* **1983**, *16*, 173.
(3) Ananthanarayanan, V. S.; Andreatta, R. H.; Poland, D.; Scheraga, H. A. *Macromolecules* **1971**, *4*, 417.
(4) Platzer, K. E. B.; Ananthanarayanan, V. S.; Andreatta, R. H.; Scheraga, H. A. *Macromolecules* **1972**, *5*, 177.
(5) Alter, J. E.; Taylor, G. T.; Scheraga, H. A. *Macromolecules* **1972**, *5*, 739.
(6) Van Wart, H. E.; Taylor, G. T.; Scheraga, H. A. *Macromolecules* **1973**, *6*, 266.
(7) Alter, J. E.; Andreatta, R. H.; Taylor, G. T.; Scheraga, H. A. *Macromolecules* **1973**, *6*, 564.
(8) Maxfield, F. R.; Alter, J. E.; Taylor, G. T.; Scheraga, H. A. *Macromolecules* **1975**, *8*, 479.
(9) Scheule, R. K.; Cardinaux, F.; Taylor, G. T.; Scheraga, H. A. *Macromolecules* **1976**, *9*, 23.
(10) Dygert, M. K.; Taylor, G. T.; Cardinaux, F.; Scheraga, H. A. *Macromolecules* **1976**, *9*, 794.
(11) Matheson, R. R.; Nemenoff, R. A.; Cardinaux, F.; Scheraga, H. A. *Biopolymers* **1977**, *16*, 1567.
(12) van Nispen, J. W.; Hill, D. J.; Scheraga, H. A. *Biopolymers* **1977**, *16*, 1587.
(13) Hill, D. J.; Cardinaux, F.; Scheraga, H. A. *Biopolymers* **1977**, *16*, 2447.
(14) Konishi, Y.; van Nispen, J. W.; Davenport, G.; Scheraga, H. A. *Macromolecules* **1977**, *10*, 1264.
(15) Kobayashi, Y.; Cardinaux, F.; Zweifel, B. O.; Scheraga, H. A. *Macromolecules* **1977**, *10*, 1271.
(16) Hecht, M. H.; Zweifel, B. O.; Scheraga, H. A. *Macromolecules* **1978**, *11*, 545.
(17) Hodges, R.; Saund, A.; Chung, P.; St.-Pierre, S.; Reid, R. *J. Biol. Chem.* **1981**, *256*, 1214.
(18) Poland, D. C.; Scheraga, H. A. *Biopolymers* **1965**, *3*, 305.
(19) Schellman, J. A. *C. R. Trav. Lab. Carlsberg., Ser. Chim.* **1955**, *29*, 230.
(20) Flory, P. J. *J. Am. Chem. Soc.* **1956**, *78*, 5222.
(21) Jacobson, H.; Stockmayer, W. H. *J. Chem. Phys.* **1950**, *18*, 1600.
(22) Poland, D.; Scheraga, H. A. "Theory of Helix–Coil Transitions in Biopolymers"; Academic Press: New York, 1970.
(23) (a) Fixman, M.; Freire, J. J. *Biopolymers* **1977**, *16*, 2693. (b) de Gennes, P.-G. "Scaling Concepts in Polymer Physics"; Cornell University Press: Ithaca, NY, 1979.
(24) Zimm, B.; Bragg, J. *J. Chem. Phys.* **1959**, *31*, 526.
(25) Mattice, W. L.; Skolnick, J. *Macromolecules* **1982**, *15*, 1088.
(26) Hodges, R.; Sodek, J.; Smillie, L.; Jurasek, L. *Cold Spring Harbor Symp. Quant. Biol.* **1972**, *37*, 299.
(27) McLachlan, A.; Stewart, M. *J. Mol. Biol.* **1975**, *98*, 293.
(28) Stone, D.; Smillie, L. *J. Biol. Chem.* **1978**, *253*, 1137.
(29) Mak, A.; Lewis, W.; Smillie, L. *FEBS Lett.* **1979**, *105*, 232.
(30) Crothers, D. M.; Kallenbach, N. R. *J. Chem. Phys.* **1966**, *45*, 917.
(31) Flory, P. "Statistical Mechanics of Chain Molecules"; Wiley: New York, 1969; Chapter 3.
(32) Holtzer, M. E.; Holtzer, A.; Skolnick, J. *Macromolecules* **1983**, *16*, 462.
(33) Lifson, S.; Roig, A. *J. Chem. Phys.* **1961**, *34*, 1963.
(34) Pato, M.; Mak, A.; Smillie, L. *J. Biol. Chem.* **1981**, *256*, 593.
(35) Poland, D. *Biopolymers* **1974**, *13*, 1859. We shall refer to equations in Poland's paper by the prefix P.

Theory of Phase Equilibria in Systems Containing Block Copolymers

Kin Ming Hong and Jaan Noolandi*

Xerox Research Centre of Canada, 2480 Dunwin Drive, Mississauga, Ontario, Canada L5L 1J9.

Received September 30, 1982

ABSTRACT: A theory for inhomogeneous multicomponent polymer systems developed earlier by the authors is simplified for the case where the inhomogeneity is weak, and this theory is used to study the phase diagrams of a mixture of block copolymers, homopolymers, and solvents. The free energy of the system is expressed as a functional of the deviations in the concentration profiles from their homogeneous values, and a perturbation expansion up to fourth order in the fluctuations is carried out. For a mixture of a block copolymer and a nonselective solvent a simple expression is derived for the inhomogeneous free energy term, and some typical phase diagrams are calculated. The existence of eutectic points, similar to those studied in metallurgy, is demonstrated. Phase diagrams for block copolymer–homopolymer systems are also discussed, and homopolymer-induced mesophase formation is predicted. The periodicity of the lamellar structure with varying homopolymer concentration is calculated, and the density profiles near demixing are shown.

1. Introduction

A polymeric blend containing block copolymers can exhibit a macroscopic phase separation as well as a microscopic one. These polymeric alloys have been intensively studied in recent years because of their remarkable structural and mechanical properties.[1-3] The phase separation behavior of such systems has also been a problem of longstanding interest to theorists.[4-15] Krause[4] has adopted a thermodynamic approach, and described the phase separations in macroscopic terms. Meier,[5,6] on the other hand, has studied the microdomain formation from a more microscopic point of view, and on the basis of these

0024-9297/83/2216-1083$01.50/0

ideas, Helfand[7,8] has developed a self-consistent theory for pure block copolymer systems. Recently, an interesting approach for dealing with very diffuse interfaces has been developed by Leibler,[9] who has studied the microphase separation transition and the stability of the various morphologies of pure block copolymers using the random-phase approximation.

In our earlier papers,[10-13] we have developed a new self-consistent theory for multicomponent systems. In this paper, we simplify the formalism in the limit where the inhomogeneity in the system is weak, with a view to studying the possible phase diagrams of a system containing block copolymers in a mixture with a solvent or a homopolymer. A brief summary of this work has been published earlier.[14] In section 2 we derive an expression for the free energy of the multicomponent system as a functional of the deviations in the concentration profiles from their homogeneous values, and we consider the simplest possible case where only homopolymers and solvents are present, with no microphase separation taking place. The more interesting case where a block copolymer is one of the components is considered in section 3, and a simple expression is derived for the inhomogeneous free energy for a mixture of a block copolymer and a nonselective solvent. Section 4 deals with a number of possible phase diagrams obtained for systems consisting of a block copolymer and another component. In particular the phenomenon of homopolymer-induced mesophase formation is discussed, and the existence of eutectic points in the phase diagrams is pointed out. The limitations of our calculations are discussed in section 5, and the Appendix shows how to deal with the case of random copolymers.

2. Free Energy as a Functional of Density

(a) General Theory. Let us consider a system containing small molecules, homopolymers, and block copolymers and study the reduced free energy per unit volume, $f = F/(\rho_0 V k_B T)$. Here, F is the total free energy of the system, V the total volume, ρ_0 some reference number density (used in the definition of the Flory–Huggins interaction parameters), k_B the Boltzmann constant, and T the absolute temperature. In this paper, we shall only consider the case of an incompressible system, which is a good approximation for polymer liquids. However, the generalization to the compressible case is straightforward as described in ref 12.

It should be noted that the formalism developed in ref 7 and 10, and used in this paper, is based on the mean-field Flory–Huggins model and, as such, cannot describe the excluded volume effect, which is important in dilute polymer solutions. However, the mean-field approximation does provide an adequate description of more concentrated solutions. Using a criterion due to de Gennes, one can estimate[10] the dividing line (not sharply defined) between dilute and concentrated solutions to be where the polymer volume fraction is about $Z^{-1/2}$, where Z is the degree of polymerization. Thus, it should be borne in mind that the mean-field approximation used in this paper is valid only when the polymer concentration is higher than $Z^{-1/2}$.

We can write the free energy of the inhomogeneous mixture in the form

$$f = f_h + \Delta f \tag{2.1}$$

where f_h is the Flory–Huggins free energy of the system in the homogeneous state

$$f_h = \sum_{\kappa}^{C} \phi_\kappa \mu_{0\kappa} + \tfrac{1}{2}\sum_{\kappa\lambda}^{C} \chi_{\kappa\lambda}\phi_\kappa\phi_\lambda + \sum_{\kappa}^{C} (\phi_\kappa/r_\kappa) \ln \phi_\kappa \tag{2.2}$$

Here ϕ_κ is the overall volume fraction of component κ, $r_\kappa = \rho_0 Z_\kappa/\rho_{0\kappa}$, where Z_κ is the degree of polymerization, $\rho_{0\kappa}$ and $\mu_{0\kappa}$ are respectively the density and chemical potential of the pure component, and $\chi_{\kappa\lambda}$ is the Flory–Huggins interaction parameter. The "C" over the summation sign indicates that a copolymer is treated as a single component. For a block copolymer C ≡ AB, we have

$$r_C = r_A + r_B \tag{2.3}$$

$$\chi_{C\kappa} = f_A\chi_{A\kappa} + f_B\chi_{B\kappa} - f_A f_B \chi_{AB} \tag{2.4}$$

where $f_A = r_A/r_C$, etc.

The second contribution, Δf, to the free energy comes from the inhomogeneity of the system and, for a system of Gaussian chains, has the form[13]

$$\Delta f = \frac{1}{2V}\sum_{\kappa\lambda}\int d^3x\, d^3y\, \chi_{\kappa\lambda}(\mathbf{x}-\mathbf{y})\psi_\kappa(\mathbf{x})\psi_\lambda(\mathbf{y}) - \frac{1}{V}\sum_{\kappa}\int d^3x\, \psi_\kappa(\mathbf{x})\omega_\kappa(\mathbf{x}) - \sum_{\kappa}^{C}\frac{\phi_\kappa}{r_\kappa}\ln(\mathcal{Q}_\kappa/V) \tag{2.5}$$

Here $\omega_\kappa(\mathbf{x})$ is the effective potential, $\psi_\kappa(\mathbf{x})$ is the deviation of the local volume fraction $\phi_\kappa(\mathbf{x})$ from the average volume fraction, i.e.,

$$\psi_\kappa(\mathbf{x}) = \phi_\kappa(\mathbf{x}) - \phi_\kappa \tag{2.6}$$

and $\chi_{\kappa\lambda}(\mathbf{x})$ is the generalization of the Flory–Huggins interaction parameter $\chi_{\kappa\lambda}$ to the nonlocal case, the two being related by the equation

$$\chi_{\kappa\lambda} = \int d^3x\, \chi_{\kappa\lambda}(\mathbf{x}) \tag{2.7}$$

$\mathcal{Q}_\kappa$ is a functional of ω_κ defined as follows: if κ = S, a homopolymer or a small molecule component, then

$$\mathcal{Q}_S = \int d^3x\, d^3y\, Q_S(\mathbf{x},1|\mathbf{y}) \tag{2.8}$$

and if κ = C ≡ AB, a block copolymer, then

$$\mathcal{Q}_C = \int d^3x\, d^3y\, d^3z\, Q_A(\mathbf{x},1|\mathbf{y})Q_B(\mathbf{y},1|\mathbf{z}) \tag{2.9}$$

with Q_κ given in terms of ω_κ by the equations[10]

$$(1/r_\kappa)(\partial/\partial t)Q_\kappa(\mathbf{x},t|\mathbf{x}_o) = \tfrac{1}{6}\hat{b}_\kappa^2\nabla^2 Q_\kappa(\mathbf{x},t|\mathbf{x}_o) - \omega_\kappa(\mathbf{x})Q_\kappa(\mathbf{x},t|\mathbf{x}_o) \tag{2.10}$$

$$Q_\kappa(\mathbf{x},0|\mathbf{x}_o) = \delta(\mathbf{x}-\mathbf{x}_o) \tag{2.11}$$

Here, $\hat{b}_\kappa^2 = \rho_{0\kappa}b_\kappa^2/\rho_0$, b_κ being the Kuhn length of the polymer κ. Note that for a small molecule component, we have $Z_S = 1$ and $b_S = 0$.

The equilibrium density profile $\psi_\kappa(\mathbf{x})$ and the effective potential $\omega_\kappa(\mathbf{x})$ are then determined by the minimization of Δf subject to the constraints

$$\sum_\kappa \psi_\kappa(\mathbf{x}) = 0 \tag{2.12}$$

$$\int d^3x\, \psi_\kappa(\mathbf{x}) = 0 \tag{2.13}$$

The first constraint comes from the condition of incompressibility while the second follows the definition of ψ_κ. Furthermore, as ω_κ can only be determined up to an additive constant, we have imposed on it the constraint

$$\int d^3x\, \omega_\kappa(\mathbf{x}) = 0 \tag{2.14}$$

to make it unique. This also ensures that ω_κ is small when the inhomogeneity is weak. Finally, it should be noted that the absence of a "C" over a summation sign indicates that the different blocks A and B of a copolymer C = AB are to be treated as separate components.

In the remainder of this section, we shall obtain an expansion of Δf in powers of ω_κ. For this purpose, it is more convenient to consider the Fourier transform of the various quantities. For example,

$$\tilde{\psi}_\kappa(\mathbf{k}) = \int d^3x\ \psi_\kappa(\mathbf{x}) e^{-i\mathbf{k}\cdot\mathbf{x}} \tag{2.15}$$

$$\tilde{Q}_\kappa(\mathbf{k},t|\mathbf{k}_0) = \int d^3x\ d^3x_0\ Q_\kappa(\mathbf{x},t|\mathbf{x}_0) e^{-i(\mathbf{k}\cdot\mathbf{x}-\mathbf{k}_0\cdot\mathbf{x}_0)} \tag{2.16}$$

and the constraints eq 2.12–2.14 now read

$$\sum_\kappa \tilde{\psi}_\kappa(\mathbf{k}) = 0 \tag{2.17}$$

$$\tilde{\psi}_\kappa(\mathbf{0}) = 0 \tag{2.18}$$

$$\tilde{\omega}_\kappa(\mathbf{0}) = 0 \tag{2.19}$$

Similarly, eq 2.5, 2.8, and 2.9 can now be written as

$$\Delta f = \frac{1}{2V}\sum_{\kappa\lambda}\int \frac{d^3k}{(2\pi)^3}\,\tilde{\chi}_{\kappa\lambda}(\mathbf{k})\tilde{\psi}_\kappa(\mathbf{k})\tilde{\psi}_\lambda(-\mathbf{k}) - \frac{1}{V}\sum_\kappa \int \frac{d^3k}{(2\pi)^3}\,\tilde{\psi}_\kappa(\mathbf{k})\tilde{\omega}_\kappa(-\mathbf{k}) - \sum_\kappa^{\mathrm{C}} \frac{\phi_\kappa}{r_\kappa} \ln (\mathcal{Q}_\kappa/V) \tag{2.20}$$

$$\mathcal{Q}_\mathrm{S} = \tilde{Q}_\mathrm{S}(\mathbf{0},1|\mathbf{0}) \tag{2.21}$$

$$\mathcal{Q}_\mathrm{C} = \int \frac{d^3k}{(2\pi)^3}\,\tilde{Q}_\mathrm{A}(\mathbf{0},1|\mathbf{k})\tilde{Q}_\mathrm{B}(\mathbf{k},1|\mathbf{0}) \tag{2.22}$$

and eq 2.10 can be solved by iteration to express $\tilde{Q}_\kappa$ explicitly as a power series of $\tilde{\omega}_\kappa$

$$\tilde{Q}_\kappa(\mathbf{k},t|\mathbf{k}_0) = \sum_{n=0}^{\infty}\frac{(-r_\kappa)^n}{n!}\int \frac{d^3k_1}{(2\pi)^3}\cdots\frac{d^3k_{n+1}}{(2\pi)^3}\times (2\pi)^3\delta(\mathbf{k} + \sum_{i=1}^{n+1}\mathbf{k}_i)(2\pi)^3\delta(\mathbf{k}_0 + \mathbf{k}_{n+1})\times G_\kappa^{(n)}(\sum_{i=1}^{n+1}\mathbf{k}_i, \sum_{i=2}^{n+1}\mathbf{k}_i,...,\mathbf{k}_{n+1};t)\tilde{\omega}_\kappa(-\mathbf{k}_1)...\tilde{\omega}_\kappa(-\mathbf{k}_n) \tag{2.23}$$

where

$$G_\kappa^{(n)}(\mathbf{q}_1,...,\mathbf{q}_{n+1};t) = n!\sum_{i=1}^{n+1}\frac{e^{-x_i t}}{\prod_{j=1}^{n+1}{}'(x_j - x_i)} \tag{2.24}$$

Here $x_i = {}^1/_6 r_\kappa \hat{b}_\kappa{}^2 q_i{}^2 = {}^1/_6 Z_\kappa b_\kappa{}^2 q_i{}^2$ and the prime over the product sign indicates that the $(j = i)$th factor is to be omitted. Note also that

$$G_\kappa^{(n)}(\mathbf{0},...,\mathbf{0};t) = t^n \tag{2.25}$$

In order to facilitate the manipulation of the equations, we introduce the following shorthand notation. We let i stand for both the species index κ_i and the wave vector $\mathbf{k}_i$, i.e., $i \equiv (\kappa_i, \mathbf{k}_i)$, and write

$$\tilde{\psi}_i \equiv \tilde{\psi}_{\kappa_i}(\mathbf{k}_i) \tag{2.26}$$

$$\tilde{\omega}_i \equiv \tilde{\omega}_{\kappa_i}(-\mathbf{k}_i) \tag{2.27}$$

$$\tilde{\chi}_{ij} = \chi_{\kappa_i\kappa_j}(\mathbf{k}_i)(2\pi)^3\delta(\mathbf{k}_i + \mathbf{k}_j) \tag{2.28}$$

Then, eq 2.20 can be written in the compact form

$$\Delta f = \frac{1}{2V}\tilde{\chi}_{ij}\tilde{\psi}_i\tilde{\psi}_j - \frac{1}{V}\tilde{\psi}_i\tilde{\omega}_i - \sum_\kappa^{\mathrm{C}}\frac{\phi_\kappa}{r_\kappa}\ln(\mathcal{Q}_\kappa/V) \tag{2.29}$$

Here the summation convention is used. That is, unless indicated otherwise, summations (and integrations) over repeated subscripts are implied. Note that we do not apply the summation convention to the index κ (hence the explicit use of the summation sign for the last term) but only to the indices i, j, etc.

With these notations, we can substitute eq 2.23 into eq 2.21 and 2.22 to obtain

$$\mathcal{Q}_\kappa/V = 1 + \frac{(-r_\kappa)^2}{2!V}g^\kappa{}_{ij}\tilde{\omega}_i\tilde{\omega}_j + \frac{(-r_\kappa)^3}{3!V}g^\kappa{}_{ijk}\tilde{\omega}_i\tilde{\omega}_j\tilde{\omega}_k + ... \tag{2.30}$$

The absence of the first-order term is a consequence of the constraint of eq 2.19. The nth-order coefficient $g^\kappa{}_{i...j}$ (n subscripts) is defined as follows:

For $\kappa = \mathrm{S}$, a homopolymer, $q^\mathrm{S}{}_{i...j}$ vanishes unless all n species indices are equal to S (i.e., $\kappa_i = ... = \kappa_j = \mathrm{S}$), in which case

$$g^\mathrm{S}{}_{i...j} = (2\pi)^3\delta(\mathbf{k}_i + ... + \mathbf{k}_j)g_\mathrm{S}{}^{(n)}(\mathbf{k}_k,...,\mathbf{k}_j) \tag{2.31}$$

where $g_\mathrm{S}{}^{(n)}$ will be defined later.

For $\kappa = \mathrm{C} \equiv \mathrm{AB}$, a block copolymer, $g^\mathrm{C}{}_{i...j}$ vanishes unless the n species indices equal either A or B, in which case, if, e.g., $\kappa_i = ... = \kappa_l = \mathrm{A}$ (m indices) and $\kappa_p = ... = \kappa_j = \mathrm{B}$ ($n - m$ indices), then

$$g^\mathrm{C}{}_{i...j} = (2\pi)^3\delta(\mathbf{k}_i + ... + \mathbf{k}_j)\times f_\mathrm{A}{}^m f_\mathrm{B}{}^{n-m} g_\mathrm{A}{}^{(m)}(\mathbf{k}_i,...,\mathbf{k}_l)g_\mathrm{B}{}^{(n-m)}(\mathbf{k}_p,...,\mathbf{k}_j) \equiv (2\pi)^3\delta(\mathbf{k}_i + ... + \mathbf{k}_j)g_{\kappa_i...\kappa_j}{}^{(n)}(\mathbf{k}_i,...,\mathbf{k}_j) \tag{2.32}$$

Finally, $g_\kappa{}^{(n)}$ is defined as the symmetrization of $\hat{G}_\kappa{}^{(n)}$ over its arguments, i.e.,

$$g_\kappa{}^{(n)}(\mathbf{k}_i,...,\mathbf{k}_n) = (1/n!)\sum_P \hat{G}_\kappa{}^{(n)}(\mathbf{k}_{P1},...,\mathbf{k}_{Pn}) \tag{2.33}$$

where $P1$, ..., Pn indicates a permutation of 1, ..., n, and $\hat{G}_\kappa{}^{(n)}$ is a rewrite of $G_\kappa{}^{(n)}$ given in eq 2.24

$$\hat{G}_\kappa{}^{(n)}(\mathbf{k}_1,...,\mathbf{k}_n) = G_\kappa{}^{(n)}(\mathbf{0},\mathbf{k}_1,\mathbf{k}_1 + \mathbf{k}_2,...,\sum_{i=1}^{n}\mathbf{k}_i;\,1) \tag{2.34}$$

Note that in particular

$$g_\kappa{}^{(1)}(\mathbf{k}) = (1 - e^{-x})/x \tag{2.35}$$

and $g_\kappa{}^{(2)}(\mathbf{k},-\mathbf{k})$ is the Debye function

$$g_\kappa{}^{(2)}(\mathbf{k},-\mathbf{k}) = 2(x - 1 + e^{-x})/x^2 \tag{2.36}$$

where $x = Z_\kappa b_\kappa{}^2 k^2/6$. In later sections we shall drop the order index (n), since the order of the coefficient should be clear from the number of arguments it carries.

Substituting eq 2.30 into eq 2.29 and expanding out the logarithm, we obtain

$$\Delta f = \frac{1}{2V}\tilde{\chi}_{ij}\tilde{\psi}_i\tilde{\psi}_j - \frac{1}{V}\tilde{\psi}_i\tilde{\omega}_i - \frac{1}{2V}\sum_\kappa^{\mathrm{C}} r_\kappa\phi_\kappa g^\kappa{}_{ij}\tilde{\omega}_i\tilde{\omega}_j + \frac{1}{6V}\sum_\kappa^{\mathrm{C}} r_\kappa{}^2\phi_\kappa g^\kappa{}_{ijk}\tilde{\omega}_i\tilde{\omega}_j\tilde{\omega}_k - \frac{1}{24V}\sum_\kappa^{\mathrm{C}} r_\kappa{}^3\phi_\kappa\left(g^\kappa{}_{ijkl} - \frac{3}{V}g^\kappa{}_{ij}g^\kappa{}_{kl}\right)\tilde{\omega}_i\tilde{\omega}_j\tilde{\omega}_k\tilde{\omega}_l + ... \tag{2.37}$$

The effective potential $\tilde{\omega}_i$ can now be eliminated by minimizing Δf with respect to $\tilde{\omega}_i$, yielding

$$\tilde{\psi}_i = -r_\kappa\phi_\kappa g^\kappa{}_{ij}\tilde{\omega}_j + {}^1/_2 r_\kappa{}^2\phi_\kappa\bar{g}^\kappa{}_{ijk}\tilde{\omega}_j\tilde{\omega}_k - {}^1/_6 r_\kappa{}^3\phi_\kappa(\bar{g}^\kappa{}_{ijkl} - (3/V)g^\kappa{}_{ij}g^\kappa{}_{kl})\tilde{\omega}_j\tilde{\omega}_k\tilde{\omega}_l + ... \tag{2.38}$$

where

$$\bar{g}^\kappa{}_{ij\cdots k} = g^\kappa{}_{ij\cdots k}[1 - (1/V)(2\pi)^3\delta(\mathbf{k}_i)] \tag{2.39}$$

the presence of the delta function being a consequence of the constraints of eq 2.18 and 2.19.

Equation 2.38 can be inverted term by term to give

$$\tilde{\omega}_i = -\frac{1}{r_\kappa\phi_\kappa}[g^\kappa]_{ij}{}^{-1}\tilde{\psi}_j + \frac{1}{2r_\kappa\phi_\kappa{}^2}[g^\kappa]_{ip}{}^{-1}[g^\kappa]_{jq}{}^{-1}[g^\kappa]_{kr}{}^{-1}\bar{g}^\kappa{}_{pqr}\tilde{\psi}_j\tilde{\psi}_k - \frac{1}{6r_\kappa\phi_\kappa{}^3}[g^\kappa]_{ip}{}^{-1}[g^\kappa]_{jq}{}^{-1}[g^\kappa]_{kr}{}^{-1}[g^\kappa]_{ls}{}^{-1}\left(\bar{g}^\kappa{}_{pqrs} - 3\bar{g}^\kappa{}_{pqt}[g^\kappa]_{tu}{}^{-1}\bar{g}^\kappa{}_{urs} - \frac{3}{V}g^\kappa{}_{pq}g^\kappa{}_{rs}\right)\tilde{\psi}_j\tilde{\psi}_k\tilde{\psi}_l \tag{2.40}$$

Substituting this into eq 2.37, we finally obtain the free

energy of the system as a functional of the concentration profiles alone. Up to the 4th order in ψ_i, we have

$$\Delta f = \frac{1}{2V}\tilde{\chi}_{ij}\tilde{\psi}_i\tilde{\psi}_j + \frac{1}{2V}\sum_{\kappa}^{C}\frac{1}{r_\kappa\phi_\kappa}[g^\kappa]_{ij}^{-1}\tilde{\psi}_i\tilde{\psi}_j - \frac{1}{6V}\sum_{\kappa}^{C}\frac{1}{r_\kappa\phi_\kappa^2}[g^\kappa]_{ip}^{-1}[g^\kappa]_{jq}^{-1}[g^\kappa]_{kr}^{-1}g_{pqr}\tilde{\psi}_i\tilde{\psi}_j\tilde{\psi}_k + \frac{1}{24V}\sum_{\kappa}^{C}\frac{1}{r_\kappa\phi_\kappa^3}[g^\kappa]_{ip}^{-1}[g^\kappa]_{jq}^{-1}[g^\kappa]_{kr}^{-1}[g^\kappa]_{ls}^{-1}\left(\frac{3}{V}g^\kappa_{pq}g^\kappa_{rs} + 3g^\kappa_{pqt}[g^\kappa]_{tu}^{-1}\bar{g}^\kappa_{urs} - g^\kappa_{pqrs}\right)\tilde{\psi}_i\tilde{\psi}_j\tilde{\psi}_k\tilde{\psi}_l \quad (2.41)$$

The equilibrium concentration profiles are then determined by the minimization of this functional. This is done in section 3 where we study the phase diagrams of a mixture consisting of a block copolymer and another component.

(b) Long-Wavelength Limit. As an illustration of the use of the expression for the free energy, consider a demixed system consisting of homopolymers and small molecules only. Near the critical point, the interfacial thickness becomes large ($\gg Z_\kappa^{1/2}b_\kappa$) so that a gradient expansion of the free energy can be made in addition to the small ψ expansion already introduced.

Keeping the gradient contributions only in the second-order terms in the free energy, we have

$$\tilde{\chi}_{\kappa\lambda}(\mathbf{k}) \simeq \chi_{\kappa\lambda}(1 - \tfrac{1}{6}\sigma_{\kappa\lambda}^2k^2) \quad (2.42)$$

where $\sigma_{\kappa\lambda}$ is the range parameter for the interaction defined by

$$\chi_{\kappa\lambda}\sigma_{\kappa\lambda}^2 = \int d^3r\, \chi_{\kappa\lambda}(\mathbf{r})r^2 \quad (2.43)$$

Expanding the Debye function, we obtain

$$[g^\kappa]_{ij}^{-1} \simeq (2\pi)^2\delta(\mathbf{k}_i + \mathbf{k}_j)(1 + Z_\kappa b_\kappa^2k_i^2/18) \quad (2.44)$$

whereas for the higher order coefficients we have simply

$$g^\kappa_{i...j} \simeq (2\pi)^3\delta(\mathbf{k}_i + ... + \mathbf{k}_j) \quad (2.45)$$

Hence, the expression for the free energy reduces to

$$\Delta f = \frac{1}{V}\int d^3r \left\{\frac{1}{2}\sum_{\kappa\lambda}\chi_{\kappa\lambda}\psi_\kappa(\mathbf{r})\psi_\lambda(\mathbf{r}) - \frac{1}{12}\sum_{\kappa\lambda}\chi_{\kappa\lambda}\sigma_{\kappa\lambda}^2\nabla\psi_\kappa(\mathbf{r})\cdot\nabla\psi_\lambda(\mathbf{r}) + \sum_\kappa\left[\frac{\hat{b}_\kappa^2}{36\phi_\kappa}|\nabla\psi_\kappa(\mathbf{r})|^2 + \frac{1}{2r_\kappa\phi_\kappa}\psi_\kappa^2(\mathbf{r}) - \frac{1}{6r_\kappa\phi_\kappa^2}\psi_\kappa^3(\mathbf{r}) + \frac{1}{12r_\kappa\phi_\kappa^3}\psi_\kappa^4(\mathbf{r})\right]\right\} \quad (2.46)$$

It may be noted that eq (2.46) is the generalization of the free energy for a two-component system obtained by Joanny and Leibler.[15] These authors have used such an expression for the free energy to study the interfacial properties of the two-component system near the critical point. However, this aspect of the problem will not be pursued here.

3. Systems Containing a Block Copolymer

For systems containing block copolymers, the long wavelength (or small k) expansion derived at the end of the previous section is no longer valid, due to the fact that the block copolymer tends to organize into structures with a dimension of the order $Z_\kappa^{1/2}b_\kappa$, so that $Z_\kappa b_\kappa^2k^2$ is of the order of unity. A detailed analysis of the microdomain structures for the case of a pure block copolymer has been carried out by Leibler,[9] using a somewhat different formalism. In this section we study the phase separation behavior of a system containing a diblock copolymer AB and another component S. The latter can be a homopolymer or a small molecule.

Let us first analyze the stability of the homogeneous system relative to small fluctuations in the concentration profiles, starting with the second-order term in the free energy

$$\Delta f_2 = \frac{1}{2V}\left(\tilde{\chi}_{ij}\tilde{\psi}_i\tilde{\psi}_j + \sum_{\kappa}^{C}\frac{1}{r_\kappa\phi_\kappa}[g^\kappa]_{ij}^{-1}\tilde{\psi}_i\tilde{\psi}_j\right) \quad (3.1)$$

Since the system contains only AB and S, we have from eq 2.17

$$\tilde{\psi}_S(\mathbf{k}) = -[\tilde{\psi}_A(\mathbf{k}) + \tilde{\psi}_B(\mathbf{k})] \quad (3.2)$$

so that

$$\Delta f_2 = \frac{1}{2V}\int\frac{d^3k}{(2\pi)^3}[a(k)|\tilde{\psi}_A(\mathbf{k})|^2 + 2b(k)\tilde{\psi}_A(\mathbf{k})\tilde{\psi}_B(-\mathbf{k}) + c(k)|\tilde{\psi}_B(\mathbf{k})|^2] = \frac{1}{2V}\int\frac{d^3k}{(2\pi)^3}[\lambda_+(k)|u(\mathbf{k})|^2 + \lambda_-(k)|v(\mathbf{k})|^2] \quad (3.3)$$

where

$$a = g_{AA}^{-1}/(r_C\phi_C) + 1/(r_S\phi_Sg_S) - 2\tilde{\chi}_{AS} \quad (3.4)$$

$$b = g_{AB}^{-1}/(r_C\phi_C) + 1/(r_S\phi_Sg_S) + \tilde{\chi}_{AB} - \tilde{\chi}_{AS} - \tilde{\chi}_{BS} \quad (3.5)$$

$$c = g_{BB}^{-1}/(r_C\phi_C) + 1/(r_S\phi_Sg_S) - 2\tilde{\chi}_{BS} \quad (3.6)$$

$$\lambda_\pm = \tfrac{1}{2}(c + a \pm \Delta) \quad (3.7)$$

$$\Delta = [(c - a)^2 + 4b^2]^{1/2} \quad (3.8)$$

$$u = [\text{sgn } b\cdot(\Delta - c + a)^{1/2}\tilde{\psi}_A + (\Delta + c - a)^{1/2}\tilde{\psi}_B]/(2\Delta)^{1/2} \quad (3.9)$$

and

$$v = [\text{sgn } b\cdot(\Delta + c - a)^{1/2}\tilde{\psi}_A - (\Delta - c + a)^{1/2}\tilde{\psi}_B]/(2\Delta)^{1/2} \quad (3.10)$$

Note that in eq 3.4–3.10, the argument $\mathbf{k}$ has been suppressed, and in eq 3.4–3.6, $g_S \equiv g_S(\mathbf{k}, -\mathbf{k})$ is the Debye function and g_{AA}^{-1}, etc., are elements of the inverse of the matrix

$$\begin{pmatrix} g_{AA} & g_{AB} \\ g_{BA} & g_{BB} \end{pmatrix} = \begin{pmatrix} f_A^2g_A(\mathbf{k}, -\mathbf{k}) & f_Af_Bg_A(\mathbf{k})g_B(\mathbf{k}) \\ f_Af_Bg_A(\mathbf{k})g_B(\mathbf{k}) & f_B^2g_B(\mathbf{k}, -\mathbf{k}) \end{pmatrix} \quad (3.11)$$

From the expression for Δf_2, it is clear that the homogeneous system is stable with respect to small local fluctuations in the concentration only if $\lambda_-(k) > 0$ for all $\mathbf{k}$. Thus the spinodal of the system with respect to microphase separation is given by the condition

$$\lambda_-(k^*(\phi, \chi), \phi, \chi) = 0 \quad (3.12)$$

where k^* is the value of k that minimizes $\lambda_-(k, \phi, \chi)$. Here we have introduced the arguments ϕ and χ to emphasize that k^* is in general a function of the composition (ϕ) and the various interaction parameters (χ) and that the equation of the spinodal (eq 3.12) is a relation between the ϕ's and the χ's.

As discussed in Leibler's work,[9] in studying the system near the spinodal (i.e., for $\lambda_-(k^*) \lesssim 0$), we need only consider components of the fluctuation with wave vector k^*. Furthermore, if we consider the microdomains to have a lamellar structure, a great simplification results in that the 3rd-order term in the free energy vanishes. This imme-

diately leads to the result that, up to and including the fourth-order term in the free energy, we can set

$$u(k^*) = 0 \tag{3.13}$$

For a system near the spinodal of microphase separation into a lamellar structure, the equilibrium concentration profiles are then given by

$$\psi_A(x) = \psi \cos k^* x \tag{3.14}$$

$$\psi_B(x) = \psi R(k^*) \cos k^* x \tag{3.15}$$

$$\psi_S(x) = -\psi[1 + R(k^*)] \cos k^* x \tag{3.16}$$

where k^* is the value of k that minimizes $\lambda_-(k)$. From now on, we take k^* to be the unit for all the wave vectors. Thus we have

$$R(1) = -[\text{sgn } b(1)]\left[\frac{\Delta(1) - c(1) + a(1)}{\Delta(1) + c(1) - a(1)}\right]^{1/2} \tag{3.17}$$

and

$$\Delta f = -\tfrac{1}{2}\alpha\psi^2 + \tfrac{1}{4}\beta\psi^4 \tag{3.18}$$

where α and β are given by

$$\alpha = \frac{\Delta(1)}{2}\frac{\Delta(1) - c(1) - a(1)}{\Delta(1) + c(1) - a(1)} \tag{3.19}$$

and

$$\begin{aligned} 16\beta = {} & \frac{1}{r_S\phi_S^3}[g_S(1,-1)]^{-4}[1 + R(1)]^4\{2[g_S(1,-1)]^2 + \\ & g_S^{-1}(2,-2)[g_S(2,-1,-1)]^2 - g_S(1,1,-1,-1)\} + \\ & \frac{1}{r_C\phi_C^3}\{2[g_{AA}^{-1}(1,-1) + 2g_{AB}^{-1}(1,-1)R(1) + \\ & g_{BB}^{-1}(1,-1)R^2(1)]^2 + \sum_{ij} g_{ij}^{-1}(2,-2)U_iU_j - \\ & \sum_{ijkl} g_{ijkl}(1,1,-1,-1)S_iS_jS_kS_l\} \end{aligned} \tag{3.20}$$

with

$$U_i = \sum_{jk} g_{ijk}(2,-1,-1)S_jS_k \tag{3.21}$$

$$\begin{aligned} S_i &= g_{AA}^{-1}(1,-1) + g_{AB}^{-1}(1,-1)R(1) \quad \text{if} \quad i = A \\ &= g_{AB}^{-1}(1,-1) + g_{BB}^{-1}(1,-1)R(1) \quad \text{if} \quad i = B \end{aligned} \tag{3.22}$$

Minimizing Δf with respect to ψ, we obtain

$$\psi^2 = \alpha/\beta \tag{3.23}$$

with the free energy given by

$$\Delta f = -(\alpha^2/4\beta) \tag{3.24}$$

With this equation we can now study the phase separation behavior of the system.

In the following, we shall assume the interaction to be sufficiently short ranged that $\tilde{\chi}_{\kappa\lambda}(k) = \chi_{\kappa\lambda}$, independent of k. We begin by studying the symmetric case where the expression for the free energy can be greatly simplified.

(a) The Symmetric Case. This is the case where the system consists of a symmetric block copolymer (i.e., $f_A = f_B = {}^1/_2$, $\hat{b}_A = \hat{b}_B$) and a nonselective solvent (i.e., $\chi_{AS} = \chi_{BS}$). We then have $a(1) = c(1)$, which immediately leads to $R(1) = -1$. That is

$$\psi_B(x) = -\psi_A(x) \qquad \psi_S(x) = 0 \tag{3.25}$$

and

$$\alpha = \chi_{AB} - 1/(r_C\phi_C)[g_{AA}^{-1}(k^*,-k^*) - g_{AB}^{-1}(k^*,-k^*)] \tag{3.26}$$

Minimizing λ_- or, equivalently, maximizing α, we find

$$\min [g_{AA}^{-1}(k^*,-k^*) - g_{AB}^{-1}(k^*,-k^*)] = 10.5 \tag{3.27}$$

at

$$r_C\hat{b}^2k^{*2} = 22.7 \tag{3.28}$$

It should be noted that these numbers are identical with the corresponding ones in Leibler's work[9] for the pure copolymer. This is to be expected since in the symmetric case the solvent is inactive and acts only as a diluent, as indicated by the fact that $\psi_S = 0$. Thus the dilution approximation applies, as should be apparent from the following scaling law for the free energy: viz., for $\psi_S = 0$, we have

$$\Delta f(\phi_C,\chi_{AB},\psi_A,\psi_B) = \phi_C\Delta f(1,\phi_C\chi_{AB},\psi_A/\phi_C,\psi_B/\phi_C) \tag{3.29}$$

Returning to eq 3.26, we see that the system goes into the mesophase for $r_C\chi_{AB}\phi \geq 10.5$, and we have

$$\alpha = \chi_{AB} - 10.5/(r_C\phi_C) \tag{3.30}$$

Substituting k^* into eq 3.20, we obtain

$$\beta = 9.79/(r_C\phi_C^3) \tag{3.31}$$

so that near the transition line

$$\phi_C \gtrsim 10.5/(r_C\chi_{AB}) \tag{3.32}$$

we have

$$\Delta f = -0.27\chi_{AB}[\phi_C - 10.5/(r_C\chi_{AB})]^2 \tag{3.33}$$

and the periodicity of the microdomain structure is given by eq 3.28 as

$$D = 1.32r_C^{1/2}\hat{b} \tag{3.34}$$

The periodicity is seen to be independent of the solvent concentration in the present work. However, a more elaborate calculation including higher order terms indicates that the periodicity decreases with solvent concentration, but such considerations are beyond the scope of this paper.

(b) The Asymmetric Case. When the solvent is selective or when the sizes of the two blocks of the copolymer are different, we do not have the simplification used in (a). Rather, the full equations (eq 3.19–3.24) have to be used. Here, maximizing α and minimizing λ_- lead to slightly different values of k^*. However, the difference vanishes at the spinodals, so that for our purposes both methods are acceptable. For convenience we have chosen the first method. In the next section we present results based on these calculations. Specifically, we consider the case where the selective "solvent" is in fact a homopolymer corresponding to one of the blocks of the copolymer.

4. Phase Diagrams

(a) The Symmetric Case. The results of the previous section, in particular eq 3.33, in conjunction with eq 2.1 and 2.2, can now be used to study the phase separation behavior of the system. In Figures 1–5 we show the phase diagrams of the block copolymer in a series of progressively better, but nonselective, solvents. The parameters we use are chosen to reveal the trends in the phase separation rather than to represent specific pairs of copolymer and solvent. We have taken all the $\rho_{0\kappa}$ to be the same so that $r_\kappa = Z_\kappa$, and for the purpose of discussion, we can regard these figures to be for the case $Z_S = 1$ and $Z_C = 200$, i.e., for a mixture of a small molecule solvent and a diblock copolymer in which each block has a degree of polymerization of 100. Thus $\chi_{AB}Z_C$ depends only on the variability of χ_{AB} and may be regarded as a temperature variable. For the purpose at hand, it is best to regard all the χ's to have

a $1/T$ dependence, so that we can write $\chi_{AS} = \chi_{BS} = \lambda\chi_{AB}$, a constant multiple of χ_{AB}, with a good solvent given by a small λ and a poor one by a large λ. In this way, the figures represent phase diagrams in the concentration (ϕ_C)–temperature ($1/T$) plane.

Figure 1a shows the phase diagram of a symmetric block copolymer in a poor, nonselective solvent ($\lambda = 10$). The solid lines indicate the boundaries of the various regions in the diagram marked M, H, HH, and HM (H for homogeneous and M for mesophase).

In the region M, the system remains as a single phase consisting of microdomains (the mesophase), whereas in the region H, the system exists as a single homogeneous phase. The boundary between M and H is the spinodal for microphase separation, given by

$$\chi_{AB}Z_C\phi_C = 10.5 \tag{4.1}$$

In this part of the phase diagram the spinodal represents the direct transition line between the mesophase, M, and the homogeneous phase, H. The continuation of the spinodal beyond the point E is indicated by the dashed line.

The boundary between M and H can be interpreted in different ways. If we focus attention on a solution with constant copolymer concentration (say $\phi_C = 0.9$) and consider the effect of changing the temperature (i.e., varying χ_{AB}), we are looking at the vertical line ($\phi_C = 0.9$) in the diagram. Suppose we start at a low temperature (say $\chi_{AB}Z_C = 20$); then the system is initially in M, a single phase with microdomains. As the temperature is raised, we move downward until the region H is reached (at $\chi_{AB}Z_C = 11.7$) and the system becomes a single homogeneous phase. Thus the transition line gives the melting curve of the microdomain structure. On the other hand, if we keep the temperature constant (say at $\chi_{AB}Z_C = 15$), then the corresponding line describes the effect of the solvent on the block copolymer. Starting from the pure block copolymer ($\phi_C = 1$) in M we move horizontally to the left as solvent is added. When the transition is reached at $\phi_C = 0.7$ or 30% solvent concentration the microdomain structure disappears. Thus the boundary line determines the amount of solvent required to dissolve the microdomain structure or, equivalently, gives the critical copolymer concentration required for microphase separation.

If we maintain the same temperature (at $\chi_{AB}Z_C = 15$) and keep on adding solvent, we have a homogeneous copolymer solution in the range $0.44 < \phi_C < 0.70$ (i.e., in region H). However, as we enter the region HH, the system demixes, with an almost pure solvent phase separating from a homogeneous polymer solution with $\phi_C = 0.44$. This is not surprising since we are dealing with a poor solvent here. The left and right boundaries of HH are the usual binodals determined by the Flory–Huggins theory. The corresponding spinodal is indicated by the dot–dashed curve.

At a temperature (say $\chi_{AB}Z_C = 20$) lower than that indicated by E ($\chi_{AB}Z_C = 17.9$) the situation is somewhat different. Here, on dilution of the concentrated polymer solution, we have a single mesophase until we enter the region HM. Then an almost pure solvent phase separates out, the remaining polymer solution is sufficiently concentrated ($\phi_C = 0.67$) that it stays in the mesophase, and the microdomain structure is not dissolved. The binodals for the region HM deviate from those determined by the Flory–Huggins theory. However, since in this particular case the polymer–solvent interaction dominates over the polymer–polymer interaction (i.e., $\lambda = 10$, $|f_h| \gg |\Delta f|$), the deviation is small, but this is not the case for the diagrams shown in the other figures.

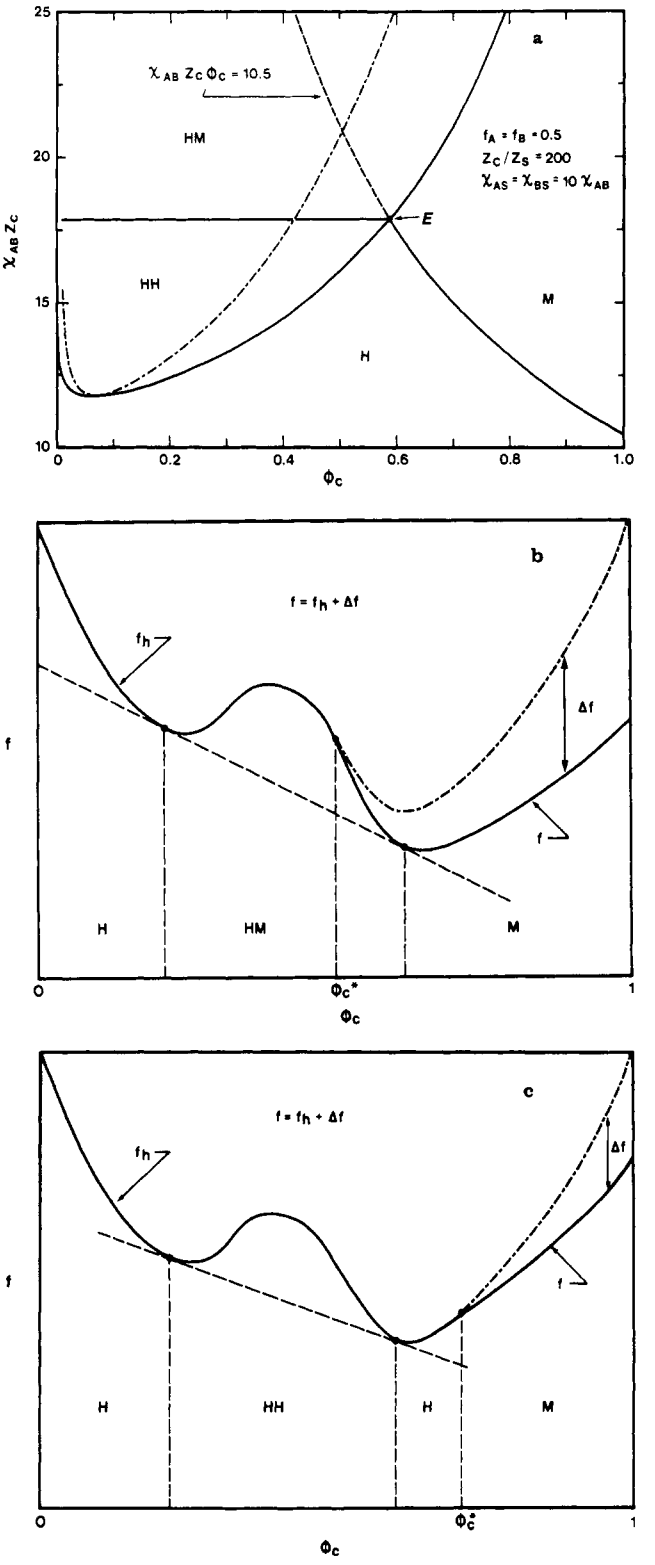

Figure 1. (a) Phase diagram of a mixture of a block copolymer and a nonselective solvent. The degree of polymerization of each block is 100, and $Z_S = 1$ for the solvent. The different regions are indicated by M (mesophase), H (homogeneous), HM (homogeneous–mesophase), and HH (homogeneous–homogeneous). E represents the *eutectic* point, as explained in the text. The solid lines enclosing the regions HM and HH are the binodals, and the solid line between M and H is the spinodal for microphase separation. The continuation of the spinodal beyond the point E is indicated by the dashed line. The dot–dashed curve shows the spinodal determined by the Flory–Huggins theory. (b) Schematic diagram of homogeneous (f_h), inhomogeneous (Δf), and total (f) free energies for $\chi_{AB}Z_C = 20$. ϕ_C^* is the smallest copolymer volume fraction for which mesophase formation is possible. (c) Schematic diagram of free energies for $\chi_{AB}Z_C = 15$.

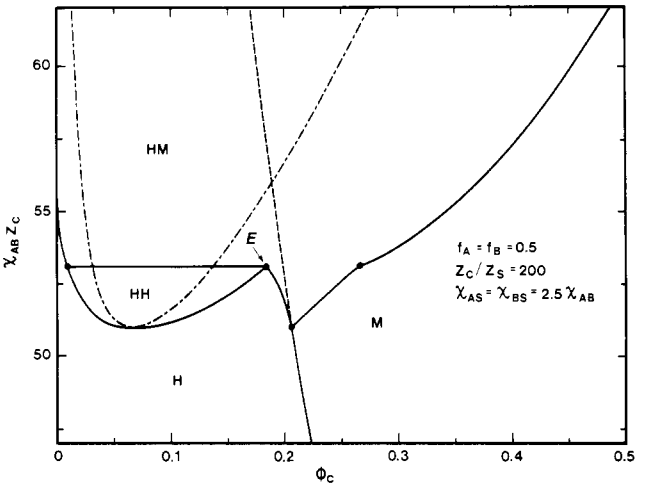

Figure 2. Phase diagram of a mixture of a block copolymer and a nonselective solvent. The same conditions as described in Figure 1 apply, except that a better solvent is assumed.

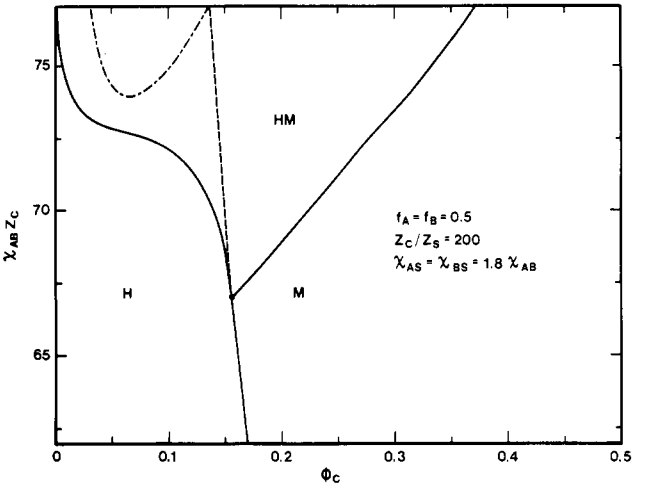

Figure 3. Phase diagram of a mixture of a block copolymer and a nonselective solvent, assumed to be better than that given in Figure 2.

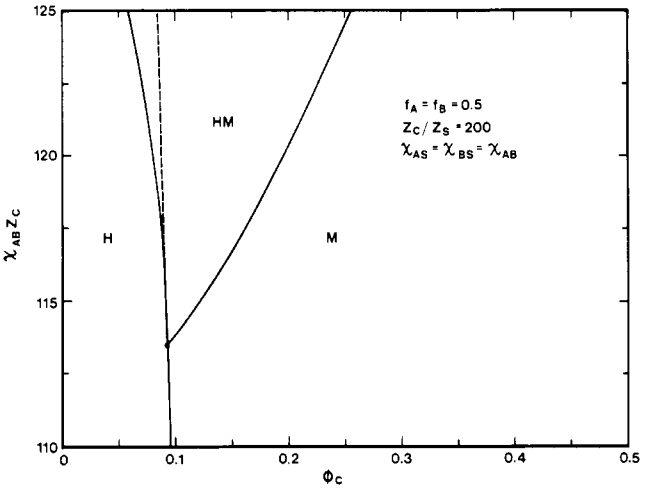

Figure 4. Phase diagram of a mixture of a block copolymer and a nonselective solvent, with all interaction parameters equal, the other conditions being the same as for Figure 1.

Finally, we note that the temperature corresponding to E ($\chi_{AB}Z_C = 17.9$) may be identified as a eutectic temperature.[14] It is the lowest temperature at which a homogeneous solution, besides the almost pure solvent, can exist. Technically speaking, at this temperature we can have three phases in equilibrium: viz., the almost pure solvent, the homogeneous polymer solution at $\phi_C = 0.59$, and the mesophase at $\phi_C = 0.59$. However, for this particular case, the latter two phases are indistinguishable. A more illustrative example of the coexistence of three distinct phases at the eutectic temperature will be discussed regarding Figure 2. The composition corresponding to E ($\phi_C = 0.59$) may be called the eutectic composition in the sense that, aside from the almost pure solvent, a mixture with concentration $\phi_C = 0.59$ remains a homogeneous solution all the way down to the eutectic temperature, whereas mixtures with other compositions would demix or undergo microphase separation earlier.

Figures 1b and 1c show, schematically, the shapes of the free energy curves, which lead to the phase separation behavior described for Figure 1a. In Figure 1b $\chi_{AB}Z_C = 20$, and the minimum value of ϕ_C (denoted by ϕ_C^*) for which the free energy of the inhomogeneous state is lower than that of the homogeneous state lies to the *left* of the point of tangency near the second minimum in f_h. It is immediately apparent that *three* regions will result in the phase diagram for $\chi_{AB}Z_C = 20$. On the other hand, if $\chi_{AB}Z_C = 15$, as in Figure 1c, ϕ_C^* lies to the right of the tangency point near the second minimum in f_h. It is clear that there will now be *four* regions in the phase diagram for $\chi_{AB}Z_C = 15$. It should also be noted that the extent of the almost pure homogeneous solvent phase has been greatly exaggerated for the sake of clarity in Figure 1c.

Figure 2 shows the phase diagram of the block copolymer in a somewhat better solvent ($\lambda = 2.5$). As can be expected, here the demixing occurs at lower temperatures (larger $\chi_{AB}Z_C$) and higher solvent concentrations. As mentioned earlier, in this case we have the possibility of three coexisting phases at the eutectic temperature ($\chi_{AB}Z_C = 53$): viz., the almost pure solvent, an 18% homogeneous polymer solution, and a 26% polymer solution in the mesophase. The eutectic point, E, has the same meaning as before. A new feature in this phase diagram is the development of a "horn" in HM below E. This means that slightly above the eutectic temperature (say at $\chi_{AB}Z_C = 52.5$) the system on dilution first demixes into a mesophase and a slightly less concentrated homogeneous phase. On further dilution, the homogeneous phase grows at the expense of the mesophase until a single homogeneous solution is obtained. Further dilution brings the system into the region HH where an almost pure solvent phase separates from the homogeneous polymer solution. The binodals of the HM region now show significant deviation from those determined by the Flory–Huggins theory. Note that the dot–dashed curve indicates the spinodal deduced from the Flory–Huggins theory only.

Figures 3 and 4 show the effect of progressively better solvents ($\lambda = 1.8$ and 1.0, respectively). Note that the demixing has been pushed to regions of higher $\chi_{AB}Z_C$ (lower temperature) and lower ϕ_C and the region HH has now disappeared.

Finally, in Figure 5a we have the case of a relatively good solvent ($\lambda = 0.3$). Here the "horn" finally gives way to an MM region. In this new region, the system demixes into two phases, but now the temperature is so low that in both phases microdomain formation is possible. Note also that here the boundary line between H and HM lies to the left but almost coincides with the spinodal for microphase separation.

Figure 5b shows the corresponding schematic free energy diagram. The value of ϕ_C^* is now so small that mesophase formation is favored for almost all copolymer compositions. In particular multimesophase formation is expected, as is evident from the figure.

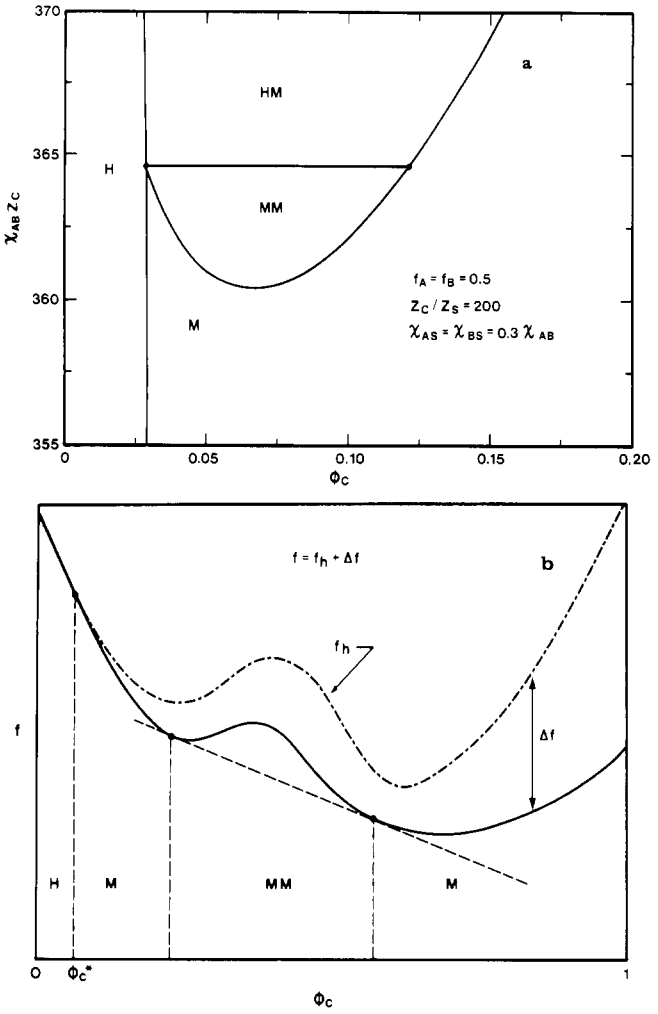

Figure 5. (a) Phase diagram of a mixture of a block copolymer and a good nonselective solvent, with all other conditions the same as for Figure 1. (b) Schematic diagram of free energies for $\chi_{AB}Z_C = 363$.

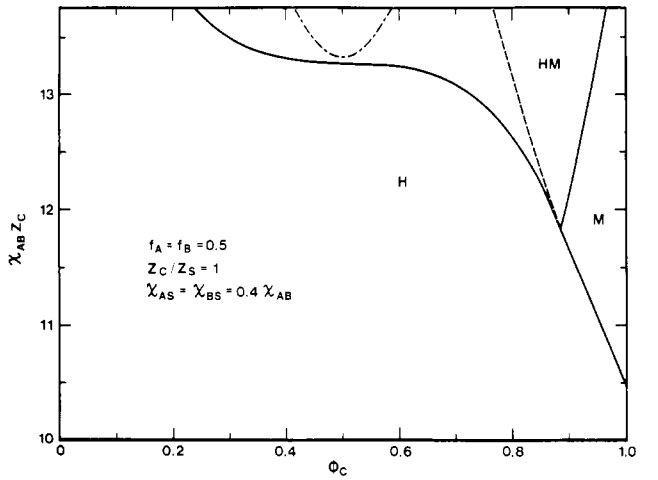

Figure 6. Phase diagram of a mixture of a block copolymer with a hypothetical homopolymer, which has the same interaction parameters with both blocks of the copolymer.

We conclude this discussion on the symmetric case by considering the situation where the nonselective "solvent" is a homopolymer. Although this example is rather academic, it serves the purpose of illustrating the effect of changing Z_S. In Figure 6 we have the case of $Z_S = Z_C$. This phase diagram can be compared with Figure 3 and illustrates the general trend that as the solvent is replaced by

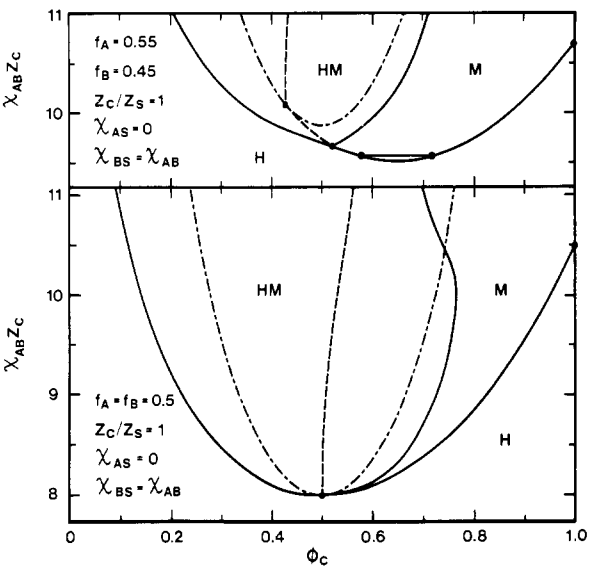

Figure 7. Top panel shows the phase diagram obtained by lengthening the A block relative to the B block of the copolymer in the mixture with the homopolymer, which in this case has the same composition as the A block of the copolymer. The bottom panel shows the corresponding phase diagram when the blocks of the copolymer have equal degrees of polymerization.

a polymer, the system phase separates more readily. Thus, demixing occurs at lower χ_{AS} and χ_{BS}, as well as at lower ϕ_S.

(b) The Asymmetric Case. In Figures 7 and 8 we show the phase diagrams of a mixture of block copolymer AB with the homopolymer A (i.e., S). The homopolymer is taken to have the same length as the copolymer, so that $Z_S = Z_C$. It should be clear that here we have $\chi_{AS} = 0$ and $\chi_{BS} = \chi_{AB}$, since S = homopolymer of A.

The upper panel of Figure 7 is for the case where the copolymer has the A block longer than the B block (f_A:f_B = 0.55:0.45). The novel feature of this phase diagram is that for a temperature range where the pure block copolymer would be in a homogeneous state ($10.7 > \chi_{AB}Z_C > 9.5$), the addition of homopolymer A to the system can induce the mixture to undergo microphase separation.[14] This kind of behavior is perhaps not completely unexpected if one recalls the phenomenon of closed miscibility gaps in certain ternary homopolymer mixtures. In that case, a pair of mutually miscible homopolymers can be induced to demix by the addition of a selective solvent, although each of the homopolymers is individually soluble in the solvent. In the present situation, we have an induced microphase separation rather than a demixing. In the region $9.7 > \chi_{AB}Z_C > 9.5$, the homopolymer first induces the formation of microdomains, but as more homopolymer is added the microdomains eventually disappear and the system returns to a single homogeneous phase. We shall give more details about this region later in the section. For $\chi_{AB}Z_C > 9.7$, the system, on addition of homopolymer A, goes from a single mesophase M into the two-phase region HM where the homopolymer separates from the copolymer, leaving the latter in the mesophase. Here again, the dashed line indicates the spinodal for microphase separation while the dot–dashed curve is the spinodal calculated from Flory–Huggins free energy alone. Note also that here, for the pure block copolymer, the microphase separation occurs for $\chi_{AB}Z_C > 10.7$ (rather than 10.5) due to the asymmetry of the block sizes.

The lower panel of Figure 7 shows the effect of lengthening the B block at the expense of the A block. As the copolymer becomes more incompatible with the homo-

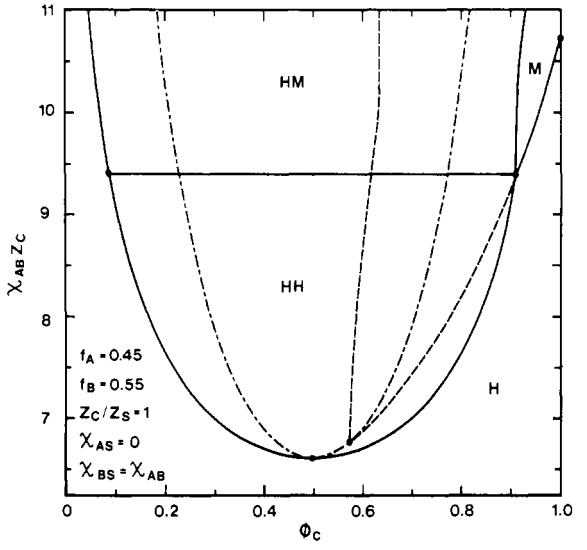

Figure 8. Phase diagram of the block copolymer–homopolymer mixture when the degree of polymerization of the B block is greater than that of the A block.

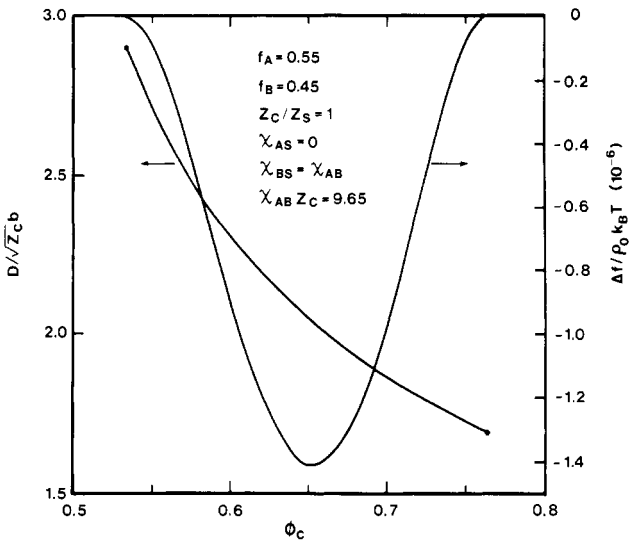

Figure 9. Plots of the free energy (relative to the homogeneous phase) and lamellar spacing for the horizontal trajectory between the two solid circles in the phase diagram shown in the upper panel of Figure 7.

polymer A, the demixing of the two occurs more readily, resulting in the expansion of the region HM. The mesophase can also accommodate a narrower range of homopolymer concentration.

Figure 8 shows the result of further lengthening the B block. A new region HH now appears in the phase diagram, indicating that for $9.4 > \chi_{AB}Z_C > 6.6$, the homopolymer simply phase separates from the copolymer without inducing microdomain formation. For $\chi_{AB}Z_C > 9.4$, microphase separation is still possible, but the mesophase can only accommodate a small amount of homopolymer, as indicated by the shrinking of the region M.

To conclude this section, let us examine in more detail the region $9.7 > \chi_{AB}Z_C > 9.5$ of the upper panel of Figure 7. Specifically, we consider the case $\chi_{AB}Z_C = 9.65$. Starting from a homogeneous phase at high copolymer concentration, induced microphase separation finally occurs at $\phi_C = 0.76$ as more and more homopolymer is added. Further addition of the homopolymer eventually causes the dissolution of the microdomains at $\phi_C = 0.54$. Figure 9 shows the lowering of the free energy (Δf) due to the microdomain formation. On the same figure is shown the periodicity

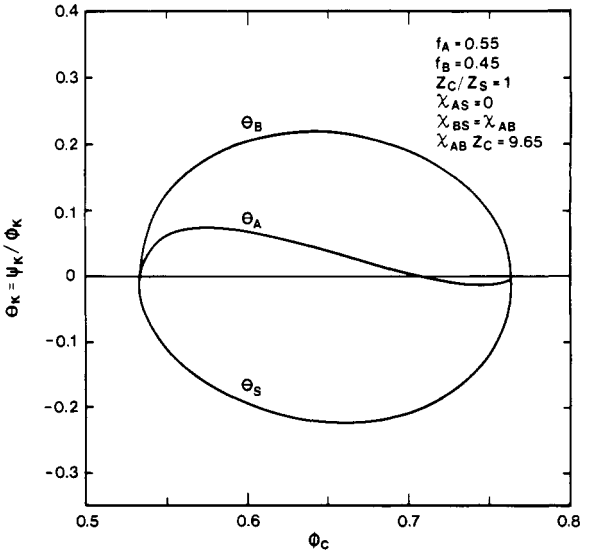

Figure 10. Amplitudes of the density profiles (ψ_κ) of each of the components as a fraction of the overall volume fractions (ϕ_κ) for the trajectory corresponding to $\chi_{AB}Z_C = 9.65$ in Figure 7 (top panel).

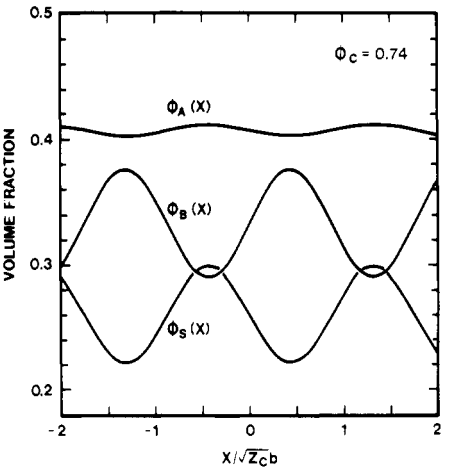

Figure 11. Density profiles of the different components for $\chi_{AB}Z_C = 9.65$ and $\phi_C = 0.74$ in the top panel of Figure 7.

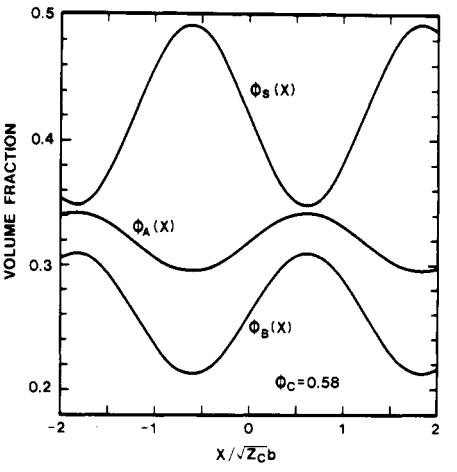

Figure 12. Density profiles of the different components for $\chi_{AB}Z_C = 9.65$ and $\phi_C = 0.58$ in the top panel of Figure 7.

D of the resulting structures, showing the thickening of the domains with increasing homopolymer concentration.

In Figure 10 we show the amplitudes of the density profile (ψ_κ) of each of the components expressed as a fraction of the overall volume fractions (ϕ_κ). Of particular

interest is the sign reversal of ψ_A at $\phi_C \simeq 0.7$. That is, for high copolymer concentrations, the density profiles of the A and B blocks are exactly out of phase as one would expect in a normal microphase separation. This is shown in Figure 11 for the concentration $\phi_C = 0.74$. At lower copolymer concentration, however, the density profiles of the two blocks are in phase, as shown in Figure 12 for $\phi_C = 0.58$. This, of course, indicates that the homopolymer is beginning to separate from the copolymer and is in fact a precursor to demixing.

5. Discussion

It should be noted that the phase diagrams presented above are based on the assumption that the mesophase exhibits lamellar structures. A more detailed analysis for the symmetric case will further partition the region M (the mesophase) into subregions exhibiting lamellar, cylindrical, and spherical structures. However, for the latter two structures, in triangular and body-centered-cubic (bccub) lattices, respectively, the third-order term in Δf does not vanish, and the analysis becomes more involved. These structures, in the case of a pure block copolymer, have been studied in detail by Leibler.[9] His results indicate that the boundary between H and M based on a bccub structure in M is in fact not too far from that based on a lamellar structure, i.e., the actual transition point is quite close to the spinodal point. The character of the transition, however, is changed from second order to first order. In our case this implies that the direct transition line between H and M opens up into a narrow two-phase HM strip. Thus, aside from these fine details and the further subdivision of the region M, it is expected that the phase diagrams described here will only be slightly modified when more accurate calculations are carried out.

The cylindrical and the spherical structures can be studied quite easily if they are placed into square and simple cubic lattices, respectively, since this only involves modifying eq 4.20 slightly. It is found (as in the case for a pure block copolymer) that the free energies based on these two structures are higher than that based on the lamellar structure, and hence we neglect them. Nevertheless, a more complete analysis involving the triangular or bccub structure is still desirable.

It should also be noted that for the asymmetric case, the region marked H can be subdivided into regions where the solution is truly homogeneous and regions where the block copolymers form micelles. An estimate of the critical micelle concentration can be given,[13] but a full description of this effect is beyond the scope of the present work.

Finally, it should be stressed that the free energy used here is obtained as an expansion in powers of ψ_κ. That is, we have implicitly made the assumption $|\psi_\kappa(x)/\phi_\kappa| \ll 1$. This is valid near the spinodal, but ψ_κ grows away from the spinodal. Figure 10 gives some idea of the magnitude of ψ_κ/ϕ_κ. Thus, away from the spinodal, the accuracy of the calculation decreases. However, the qualitative features of the phase diagrams should remain the same. An interesting application of this theory should be to the recent experimental work of Roe et al.,[16] who have studied the phase diagrams of polystyrene–polybutadiene block copolymers blended with the corresponding homopolymers.

Acknowledgment. Jaan Noolandi thanks Prof. C. Wippler and the staff at the Centre de Recherches sur les Macromolecules, Strasbourg, France, for their kind hospitality during the summer of 1981. He also thanks Prof. H. Benoit and Dr. L. Leibler for helpful discussions during the initial stages of this work.

Appendix

In this appendix we outline briefly how random copolymers can be treated within the present formalism.

For a copolymer C, composed of monomer units of various species (λ), we have in general

$$\mathcal{Q}_C = \int d^3x\, d^3x_0\, Q_C(\mathbf{x},1|\mathbf{x}_0) \tag{A.1}$$

where $Q_C(\mathbf{x},t|\mathbf{x}_0)$ is given by

$$\frac{1}{Z_C}\frac{\partial Q_C}{\partial t} = \frac{b^2(t)}{6}\nabla^2 Q_C - \omega_C(\mathbf{x},t)Q_C \tag{A.2}$$

$$Q_C(\mathbf{x},0|\mathbf{x}_0) = \delta(\mathbf{x} - \mathbf{x}_0) \tag{A.3}$$

Here

$$\omega_C(\mathbf{x},t) = \sum_\lambda s_\lambda(t)(\rho_0/\rho_{0\lambda})\omega_\lambda(\mathbf{x}) \tag{A.4}$$

$$b^2(t) = \sum_\lambda s_\lambda(t) b_\lambda^2 \tag{A.5}$$

and $s_\lambda(t)$ is a stochastic function defined by

$$\begin{aligned} s_\lambda(t) &= 1 \text{ if the } Z_C t \text{ unit belongs to species } \lambda \\ &= 0 \text{ otherwise} \end{aligned} \tag{A.6}$$

Note that $\sum_\lambda s_\lambda(t) = 1$. For simplicity we assume all the Kuhn lengths b_λ to be the same, so that $b(t) = b_\lambda$ is independent of t.

Consistent with the continuum approximation used throughout the theory, $s_\lambda(t)$ can be replaced by its average value, $p_\lambda(t) = \overline{s_\lambda(t)}$ = probability that the $Z_C t$ unit belongs to species λ. For a diblock copolymer C = AB, $p_A(t)$ is a step function:

$$\begin{aligned} p_A(t) &= 1 \text{ for } t < Z_A/Z_C \\ &= 0 \text{ for } t > Z_A/Z_C \end{aligned} \tag{A.7}$$

whereas for a tapered copolymer, $p_A(t)$ goes smoothly from 1 to 0 as t goes from 0 to 1. For a random copolymer $p_A(t) = p_A$ is independent of t and so is $\omega_C(\mathbf{x},t) = \omega_C(\mathbf{x})$. Whatever the case, a series solution of Q_C similar to eq 2.23 can be written down, and an expansion of $\mathcal{Q}_C$ (eq 2.30) can be obtained. Of course the coefficients $g^C_{i\ldots j}$ now depend on the composition profile $p_\lambda(t)$ of the copolymer chain.

The situation is simpler when $p_\lambda(t)$ is piecewise constant. As an illustration we consider the case of a diblock copolymer where the two blocks, a and b, are themselves random copolymers of A and B, but with different compositions

$$\begin{aligned} p_A(t) &= p_a \text{ for } t < Z_a/Z_C \\ &= p_b \text{ for } t > Z_a/Z_C \end{aligned} \tag{A.8}$$

Defining

$$\frac{1}{\rho_{0a}} = \frac{p_a}{\rho_{0A}} + \frac{1 - p_a}{\rho_{0B}} \tag{A.9}$$

$$\hat{p}_a = p_a\frac{\rho_{0a}}{\rho_{0A}} \tag{A.10}$$

$$\omega_a(\mathbf{x}) = \hat{p}_a\omega_A(\mathbf{x}) + (1 - \hat{p}_a)\omega_B(\mathbf{x}) \tag{A.11}$$

and using similar definitions for ρ_{0b}, $\hat{p}_b$, and ω_b, we see that $\mathcal{Q}_C$ is given by eq 2.9 with A and B replaced by a and b, while Q_a and Q_b are given by eq 2.10, with κ = a and b, respectively.

Furthermore, writing

$$\phi_A(\mathbf{x}) = \hat{p}_a\phi_a(\mathbf{x}) + \hat{p}_b\phi_b(\mathbf{x}) \tag{A.12}$$

$$\phi_B(\mathbf{x}) = (1 - \hat{p}_a)\phi_a(\mathbf{x}) + (1 - \hat{p}_b)\phi_b(\mathbf{x}) \tag{A.13}$$

and substituting this into eq 2.1 we find that the species

indices A and B can be completely replaced by the block indices a and b, leaving the formula for the free energy unchanged. However, the interaction parameters are now given by the well-known composition rules

$$\chi_{ab} = (\hat{p}_a - \hat{p}_b)^2\chi_{AB} \quad (A.14)$$

$$\chi_{\kappa a} = \hat{p}_a\chi_{\kappa A} + (1 - \hat{p}_a)\chi_{\kappa B} - \hat{p}_a(1 - \hat{p}_a)\chi_{AB} \quad (A.15)$$

with a similar equation for $\chi_{\kappa b}$ (cf. eq 2.4). That is, a random block can be treated exactly the same way as a normal block if the above effective interaction parameters are used.

References and Notes

(1) Ramos, A. R.; Cohen, R. E. *Polym. Eng. Sci.* **1977**, *17*, 639.
(2) Eastmond, G. C.; Phillips, D. G. *Polymer* **1979**, *20*, 1501.
(3) Riess, G.; Kohler, J.; Tournut, C.; Banderet, A. *Rubber Chem. Technol.* **1969**, *42*, 447.
(4) Krause, S. In "Block and Graft Copolymers"; Burke, J. J., Weiss, V., Eds.; Syracuse University Press: Syracuse, NY, 1973.
(5) Meier, D. J. *Polym. Prepr., Am. Chem. Soc., Div. Polym. Chem.* **1970**, *11*, 400.
(6) Meier, D. J. *Polym. Prepr., Am. Chem. Soc., Div. Polym. Chem.* **1977**, *18*, 340.
(7) Helfand, E. *Macromolecules* **1975**, *8*, 552.
(8) Helfand, E.; Wasserman, Z. R. *Macromolecules* **1980**, *13*, 994.
(9) Leibler, L. *Macromolecules* **1980**, *13*, 1602.
(10) Hong, K. M.; Noolandi, J. *Macromolecules* **1981**, *14*, 727.
(11) Noolandi, J.; Hong, K. M. *Ferroelectrics* **1980**, *30*, 117.
(12) Hong, K. M.; Noolandi, J. *Macromolecules* **1981**, *14*, 1229.
(13) Noolandi, J.; Hong, K. M. *Macromolecules* **1982**, *15*, 482.
(14) Noolandi, J.; Hong, K. M. *Polym. Bull. (Berlin)* **1982**, *7*, 561.
(15) Joanny, J. F.; Leibler, L. *J. Phys. (Orsay, Fr.)* **1978**, *39*, 951.
(16) Roe, R.-J.; Zin, W.-C.; Fishkis, M. Proceedings of IUPAC Meeting, Amherst, MA, July 12–16, 1982, p 662.

Ordered Structure in Block Polymer Solutions. 4. Scaling Rules on Size of Fluctuations with Block Molecular Weight, Concentration, and Temperature in Segregation and Homogeneous Regimes

Takeji Hashimoto,* Mitsuhiro Shibayama, and Hiromichi Kawai

Department of Polymer Chemistry, Faculty of Engineering, Kyoto University, Kyoto 606, Japan.

Received September 17, 1982

ABSTRACT: The small-angle X-ray scattering (SAXS) technique with a position-sensitive detector and a 12-kW rotating-anode X-ray generator was used to study the microdomain size or wavelength of the spatial fluctuations of the A and B segments in AB diblock polymers as a function of the total degree of polymerization of the block polymers (Z), polymer volume concentration (ϕ_P), and temperature (T) in neutral solvents, i.e., solvents good for both A and B block polymers. The block polymers studied were polystyrene–polyisoprene (SI) diblock polymers having about equal block molecular lengths, thus having alternating lamellar microdomains with a lamellar identity period of D in the solutions in the segregation regime. It was found that in the segregation limit D scales as $D/b \sim Z^{2/3}(\phi_P/T)^{1/3}$ or $D/b \sim Z^{1/2}(x/x_c)^{1/3}$, where $x \equiv \phi_P/T$, $x_c \equiv (\phi_P/T)_c$, b is Kuhn's statistical segment length, and $(\phi_P/T)_c$ is the critical value of ϕ_P/T at which the microdomains are dissolved into a homogeneous mixture. At high temperatures ($T > T_c$) or low concentrations ($\phi_P < \phi_c$), the microdomains are dissolved into a homogeneous mixture. The following results were obtained in the homogeneous regime. (i) There exists a scattering maximum, the peak position of which yields the Bragg spacing D. (ii) The scattering can be adequately described in the context of the random phase approximation (RPA) proposed by de Gennes and Leibler. (iii) D satisfies a scaling rule completely different from that obtained for the segregation limit: $D/b \sim Z^{1/2+\beta}(\phi_P/T)^0$ (in the homogeneous regime), where β is related to a small excluded volume effect that exists in the concentrated solutions.

I. Introduction

If two polymers A and B have different cohesive energy densities, they tend to segregate themselves into their respective domains in the segregation limit to result in phase separation. However, due to the *molecular constraint* that A and B chains are covalently bonded in AB or ABA block polymers, the phase separation is restricted to the molecular dimensions, giving rise to *microdomains* whose sizes are controlled by the block molecular weight. This is the phenomenon that is well-known as *microphase separation*.

The physics of flexible, long-chain molecules in such a microdomain system has been extensively explored both theoretically[1-6] and experimentally.[7-10,25] It was borne out that the chains can be essentially described as random flight chains with two important *physical constraints*: (i) *uniform space-filling* with the segments in space and (ii) the *confined volume* effect. The former constraint arises from *incompressibility* of polymeric liquid, the total segment density being kept uniform everywhere in the domain space. The latter constraint arises from the repulsive interactions of the polymers A and B, A (B) chains being likely confined in A (B) domain space.

The degree of the spatial confinement is a function of the effective repulsive potential between the A and B block polymer molecules and hence is a function of temperature and concentration of the polymers if the solvent exists in the system. The theme in this paper and of some of our earlier papers[11-14] is focused on this effect of the degree of the spatial confinement of the chains on the microdomain size or spatial fluctuations of density of the A or B segments in both segregation and homogeneous regimes.

When the temperature is raised above the *thermodynamic transition temperature* (T_c) or the concentration of the polymer is lowered below the *critical concentration* (C_c), the effective repulsive potential or effective Flory–Huggins χ parameter (χ_{eff}) becomes lower than the critical value $\chi_{eff,c}$ required for maintaining the microphase-separated domain structure, resulting in an *order-to-disorder transition*,[11] i.e., the transition involving dissolution of

0024-9297/83/2216-1093$01.50/0